CERES CER_CRS_TRMM-PFM-VIRS_Edition2C
Data Quality Summary

Investigation:	**CERES**
Data Product:	**Clouds and Radiative Swath (CRS)**
Data Set:	**TRMM-PFM-VIRS (Instruments: CERES-PFM, VIRS)**
Data Set Version:	**Edition2C**

The purpose of this document is to inform users of the accuracy of this data product as determined by the CERES (Wielicki et al., 1996) Science Team. This document briefly summarizes key validation results, provides cautions where users might easily misinterpret the data, provides links to further information about the data product, algorithms, and accuracy, and gives information about planned data improvements. This document also automates registration in order to keep users informed of new validation results, cautions, or improved data sets as they become available.

This document is a high-level summary and represents the minimum necessary information for scientific users of this data product.

Table of Contents

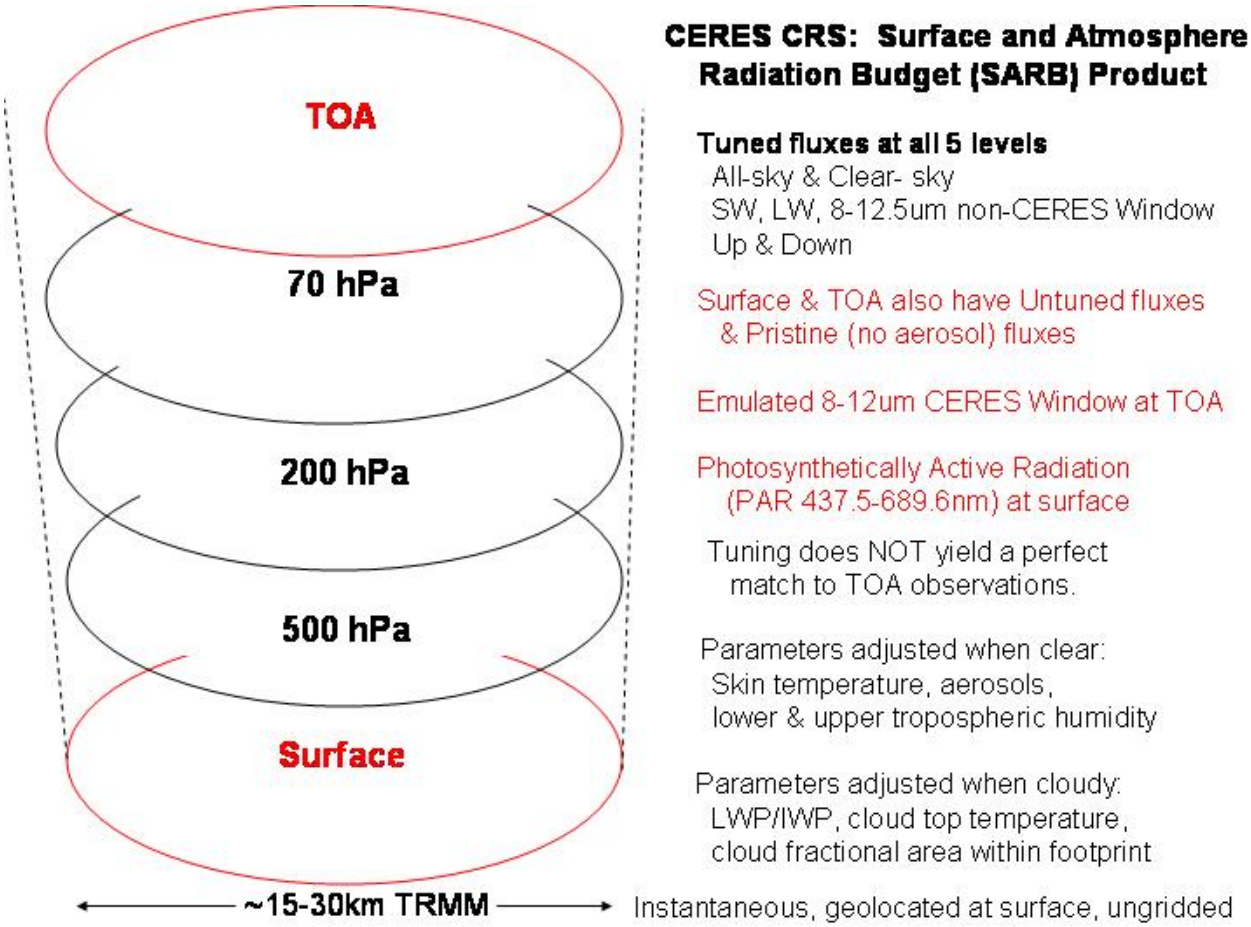

Figure 1 CRS: CERES Surface and Atmosphere Radiation Budget (SARB) product

Nature of the CRS Product

Introduction

The CRS product (Figure 1) is designed for studies of the energy balance within the atmosphere, as well as climate studies which require fields of clouds, humidity and aerosol that are consistent with radiative fluxes from the surface to the Top Of the Atmosphere (TOA). CRS software is developed and managed by the CERES Surface and Atmospheric Radiation Budget (SARB) Working Group (WG). Like its parent Single Scanner Footprint (SSF), CRS corresponds to an instantaneous CERES broadband footprint. The footprint has nominal nadir resolution of 10 km for half power points but is larger at other view angles (Figure 2). The major inputs (Figure 3) to the CRS software are the instantaneous scene identification, cloud and aerosol properties from the VIRS cloud imager pixels (nominal resolution of 1 km), and TOA radiation (from the CERES instrument) contained on the respective SSF footprint; along with 6-hourly gridded fields of temperature, humidity, wind, and ozone, and climatological aerosol data contained on the Meteorological, Ozone, and Aerosol (MOA) product. MOA products used in the production of Edition2C CRS product contain meteorological data provided by the European Center for Medium-Range Weather Forecasts (ECMWF, Rabier et al., 1998) and Stratospheric Monitoring Group Ozone Blended Analysis (SMOBA, Yang et al., 2000) ozone profiles from NCEP. In cloudy footprints, most of the aerosol data is taken from the NCAR Model for Atmospheric Transport and Chemistry (MATCH, an assimilation that employs AVHRR, see Collins et al., 2001). The CRS product contains the SSF input data; through-the-atmosphere radiative flux profiles calculated by SARB algorithms that partially constrain to CERES TOA observations; adjustments to key input parameters (i.e., optical depth for cloudy footprints and skin temperature for clear footprints); and diagnotic parameters. CRS fluxes are produced for shortwave (SW), longwave (LW), the 8.0-12.0 µm window (WN), both upwelling and downwelling at TOA, 70 hPa, 200 hPa, 500 hPa, and the surface (Figure 3). To permit the user to infer cloud forcing and direct aerosol forcing, we include surface and TOA fluxes that have been computed for cloud-free (clear) and aerosol-free (pristine) footprints. Charlock et al. (2002) compare time series of computed fluxes at TOA with CERES observations and illustrate how the flux profiles are related to the tropical circulation. Rutan et al. (2002) point out that the present results do not support "anomalous absorption" of SW by clouds. Rose and Charlock (2002) note further advances in the radiative transfer code.

A full definition of each parameter will be contained in the CRS Collection Guide, which has not been written yet. The present lengthy document should make the definitions clear to a reader having the CRS Data Product Catalog in hand. Informal extensions to the CRS Data Quality Summary will be posted under "CRS Advice" at the CAVE web site.

The SSF parent of this data set is CER_SSF_TRMM-PFM-VIRS_Edition2B. Parameters CRS-1 through CRS-131 are equivalent to SSF parameters SSF-1 through SSF-131. See SSF Data Products Catalog (PostScript). Before using these parameters, please consult the SSF Quality Summary. Definitions of these parameters are available in the SSF Collection Guide.

When referring to a CERES data set, please include the satellite name and/or the CERES instrument name, the data set version, and the data product. Multiple files which are identical in all aspects of the filename except for the 6 digit configuration code (see Collection Guide - when available) differ little, if any, scientifically. Users may, therefore, analyze data from the same satellite/instrument (here the TRMM satellite, which has a specific model of the CERES instrument named PFM), data set version (here Edition2C), and data product (here CRS)

without regard to configuration code. This CRS data set may be referred to as "CERES TRMM Edition2C CRS".

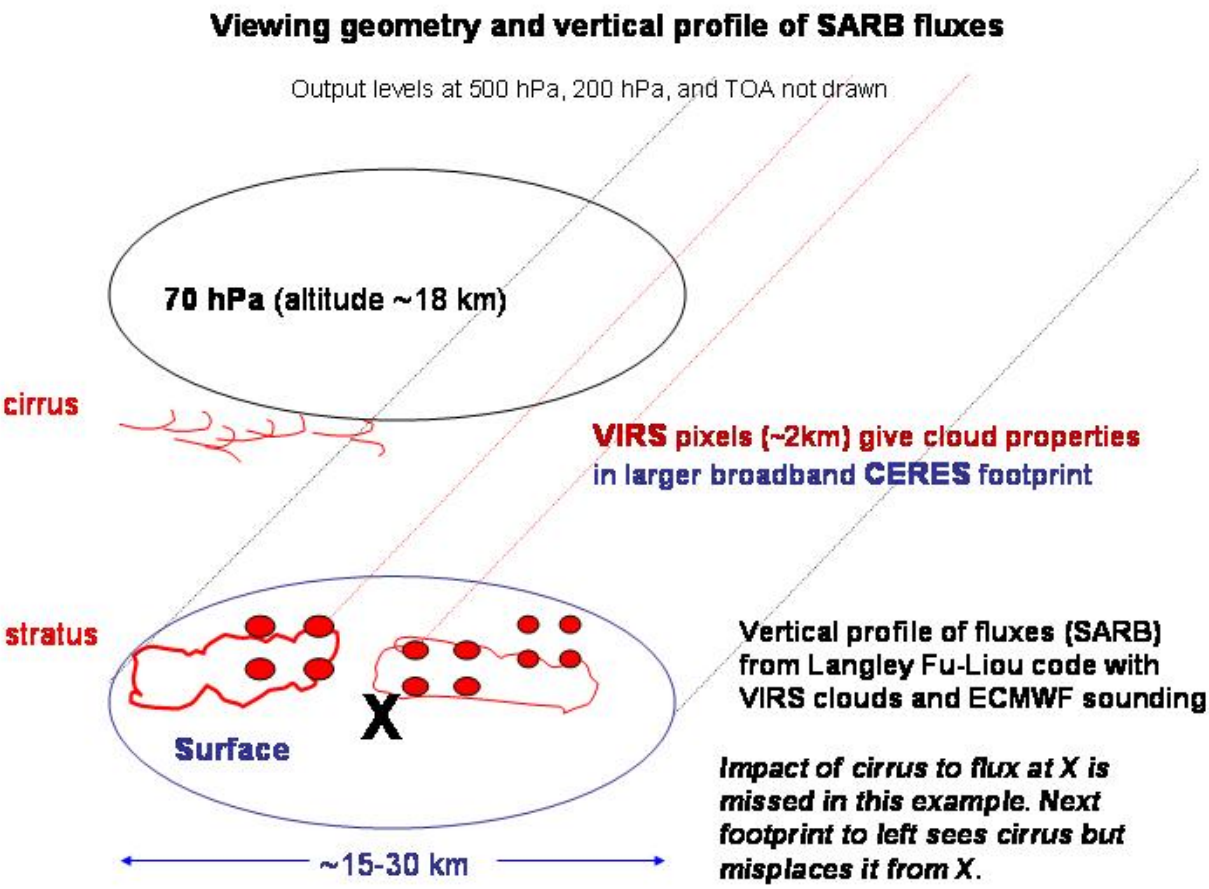

Figure 2: Typical viewing geometry with small VIRS pixels within large CERES footprints

Constrainment (tuning)

In short, the SARB flux profile in the CRS product is the output of a highly modified Fu and Liou (1993) radiative transfer code. The code is run at least twice for each broadband CERES footprint, in order to adjust inputs that determine the vertical profile of radiative fluxes. The constrainment (or tuning) algorithm does NOT yield a perfect match to CERES broadband observations at TOA. Constrainment (Rose et al. 1997; Charlock et al. 1997) is an approach to minimize the normalized, least squares differences between (1) computed TOA parameters and adjusted values for key inputs and (2) observed TOA parameters and initial values for key inputs. The algorithm assigns an a priori numerical "sigma" (uncertainty) to each TOA parameter and key input parameter. The "sigmas" for TOA parameters (first group in Table 1) are the anticipated rms differences between observations based on the core CERES instrument and the outputs of radiative transfer calculations. The sigmas for key input parameters (the second and third groups labled "cloud" and "other" in Table 1) are the anticipated rms differences between the initial (untuned) and final values of those key input parameters (tuned).

The inputs for radiative transfer calculations are depicted in Figure 3. The initial values of cloud parameters are taken from the SSF; they are narrowband imager-based retrievals of cloud properties. Initial values of other key input parameters such as PW and UTH are based on ECMWF. Initial values of AOT are taken from either the VIRS-based retrievals on SSF or from the MATCH assimilation. VIRS retrievals of AOT are available during daylight over the ocean, provided that the footprint is not heavily clouded or suspected to be contaminated by sunglint. When AOT is not available from VIRS, MATCH is used.

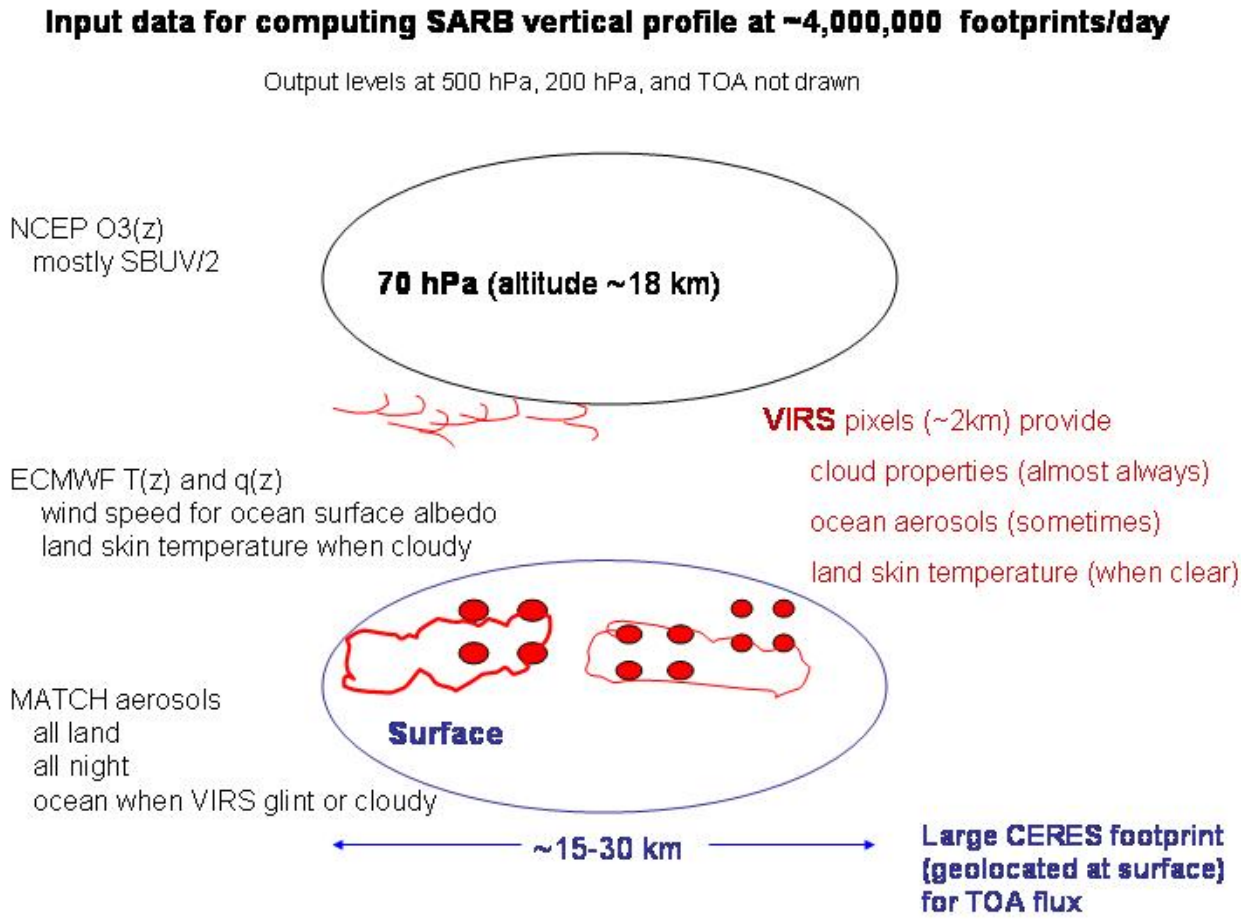

Figure 3. Inputs for determining the Surface and Atmosphere Radiation Budget (SARB)

If the reported fraction of cloudiness on the SSF file exceeds 0.05, the values of the third group of "other" (Table 1) parameters are frozen. The cloud optical depth, cloud fractional area, and cloud top height (second group in Table 1) are adjusted instead. Cloud optical depth is modified by adjusting liquid water path (LWP) or ice water path (IWP), rather than droplet or crystal size.

If the reported fraction of cloudiness on the SSF file is less than 0.05, the cloud parameters (second group in Table 1) are frozen, and the constrainment algorithm adjusts parameters from the third ("other") group in Table 1. For such clear and almost clear footprints over the ocean (note "ocean" column at the bottom of Table 1), the constrainment adjusts the surface skin temperature, lower tropospheric humidity (LTH), upper tropospheric humidity (UTH), and aerosol optical thickness (AOT). For such clear and almost clear footprints over land, the surface albedo is also adjusted; and the sigma (a priori uncertainty) for skin temperature is increased, causing a larger adjustment in skin temperature over land than over ocean. The SARB algorithm does not adjust temperature above the surface.

Every CRS footprint has TOA parameters (first box in Table 1) with observed values taken from SSF, untuned values from the initial run of the Fu-Liou code, and tuned values from the constrainment process. Every CRS footprint has input values for cloudy parameters (second box in Table 1) which are taken from SSF. and "other" parameters (third box in Table 1); and it has slots for the adjustments to each of these parameters by the constrainment process. This is summarized in Figure 1. For a discussion of observed TOA parameters (first box in Table 1) or unadjusted cloudy or clear parameters (second and third boxes in Table 1), note the SSF TRMM Edition2B Quality Summary.

What is the implication of an assigned sigma of 1.0% for broadband LW flux versus 2.0% for window WN flux versus 5.0% for filtered window radiance (top group in Table 1)? Among those 3 parameters, broadband LW flux (OLR) has the smallest sigma. Thus OLR is the tightest constraint among those 3 parameters. Adjustable parameters like cloud optical depth and surface skin temperature are pulled more toward new values causing a better match between computed and observed OLR (sigma 1%), than they are pulled to new values causing a better match between computed and observed filtered window radiance (sigma 5%). The large sigmas of 5% for the broadband LW and filtered window radiances in Table 1 in fact produce hardly any adjustments in direct response to the radiances. The smallest sigmas (1%) are assigned to broadband reflected SW and to broadband LW fluxes, as they are the primary earth radiation budget (ERB) observables. If we had less confidence in the inversion from radiance ($Wm^{-2}sr^{-1}$) to flux (Wm^{-2}) on the CERES SSF record, the sigmas of broadband LW flux and broadband LW radiance could hypothetically be reversed. There is no sigma for reflected SW radiance because our fast radiative transfer code does not simulate SW radiance.

Table 1: The a priori uncertainty ("sigma") for each adjustable parameter in the constrainment (tuning) algorithm
that produces the Surface and Atmosphere Radiation Budget (SARB) for CERES footprints

Observed by CERES at TOA (SSF record)			
TOA parameters	**Sigma (%)**	**Minimum sigma (MKS)**	**Parameter**
	1.0 %	2.0 Wm^{-2}	reflected SW flux

	1.0 %	2.0 Wm^{-2}	broadband LW flux
	2.0 %	1.0 Wm^{-2}	window WN flux
	5.0 %	0.3 Wm^{-2} sr^{-1}	broadband LW radiance
	5.0 %	0.3 Wm^{-2} sr^{-1}	filtered window radiance
From VIRS imager (SSF record)			
Cloud parameters	**Sigma**		**Adjustable parameter**
	0.15		d ln(τ) τ = optical depth
	2.0		cloud top temperature
	0.05		total cloud fraction in footprint
	0.025		fraction swap of 2 types in footprint (i.e., increase Cu and decrease Ci)
From various sources			
Other parameters	**Ocean**	**Land**	**Adjustable parameter**
	1.0 K	4.0 K	surface skin temperature
	0.15	0.10	d ln(PW) PW: surface to 500 hPa
	0.15	0.10	d ln(UTH) upper tropos. humidity
	0.002	0.015	surface albedo
	0.50	0.10	d ln(τ) aerosol optical depth

Definitions of SW, LW, and Window

CERES geophysical products define SW (shortwave or solar) and LW (longwave or thermal infrared) in terms of physical origin, rather than wavelength. We refer to the solar energy which enters and exits (overwhemingly by reflection) the earth-atmosphere system as SW. LW is regarded as the thermal energy which is emitted by the earth-atmosphere system. There is no wavelength of demarcation, for which all radiation at shorter (longer) wavelengths is called SW (LW). Thus defined, roughly 1% of the incoming SW is at wavelengths longer than 4 µm. A small amount of radiation from the sun enters the troposphere at 10 µm. This too is regarded as SW, and we strive to account for it in successive SW products. Less than 1 Wm^{-2} of OLR is at wavelengths below 4 µm. If the radiation was originally emitted by a thermal process in the earth-atmosphere system, we regard it as LW, even if it is subsequently scattered. When a small amount of thermal radiation is emitted from the surface of the Sahara at 6 µm, and a portion of that is scattered upward to space through a cirrus cloud, said portion is regarded as LW. The 8.0-12.0 µm window (WN) products are a repository of the thermal radiation in the window. We strive to eliminate any signal of solar contamination in an 8.0-12.0 µm window or broadband LW product.

The official CERES window (WN) spans 8.0 µm to 12.0 µm (1250 cm^{-1} to 833.333 cm^{-1}). The TOA observed SSF window products use this interval, as do the TOA emulated window products. CRS users should be aware that the vertical profiles of window flux (these have dimension of 5, representing surface, 500 hPa, 200 hPa, 700 hPa, and TOA) use a DIFFERENT spectral interval, 8.0 µm to 12.5 µm (1250 cm^{-1} to 800 cm^{-1}), as explained in the next section.

Radiative Transfer Code

CRS uses a fast, plane parallel correlated-k radiative transfer code (Fu and Liou, 1993, Fu et al., 1998, 1999). An economical 2 stream calculation is used for SW. The LW calculation employs a 2/4 stream version, wherein the source function is evaluated with the quick 2-stream approach, while radiances are effectively computed at 4 streams. Constituents for the thermal infrared include H_2O, CO_2, O_3, CH_4 and N_2O. A special treatment of the CERES 8.0-12.0 µm window includes CFCs (Kratz and Rose, 1998) and uses the Clough CKD 2.4 version of the H_2O continuum (the orginial Fu-Liou employed the Roberts continuum). In collaboration with Dr. Qiang Fu, the Fu-Liou code was modified to include 10 separate bands between 0.2-0.7 µm to better account for the interaction of Rayleigh scattering, aerosols, and absorption by O_3 and a minor band of H_2O. In the near IR, the code computes absorption due to H_2O. Absorption in the near IR by CO_2 and O_2 is handled as an off-line correction with the Chou and Suarez (1999) parameterization. The original code included SW from 0.2 to 4 µm. We now cover the SW at wavelengths larger than 4 µm by simply stuffing the solar insolation beyond 4 µm into a near IR band with strong absorption by H_2O. Downwelling solar photons larger than 4 µm are then mostly absorbed by the model before reaching the middle troposphere. Scattering by cloud particles, aerosols, and a non-black surface is parameterized in LW, as well as SW. For example, the desert surface has reduced thermal emission as it is non-black. As its emissivity is less than unity, the reduction in upward LW emitted by the surface is partly compensated by reflection of the downwelling LW to the surface. The code has been extended with a new band to cover thermal

emission from 2200-2850 cm^{-1}.

The Fu-Liou code covers the window with 3 bands from 8.0 µm to 12.5 µm (1250 cm^{-1} to 800 cm^{-1}); window flux vertical profiles (CRS parameters having dimension of 5 for the sequence representing the surface, 500 hPa, 200 hPa, 70 hPa, and TOA) use this interval. A different window interval, 8.0 µm to 12.0 µm (1250 cm^{-1} to 833.333 cm^{-1}), is used for TOA observations on SSF and for the formal TOA emulations on CRS-182 through CRS-185. The 8.0 µm to 12.0 µm TOA window parameters on SSF are emulated (modeled) as follows with the Fu-Liou code. First, the code produces window radiance and flux for 8.0 µm to 12.5 µm at TOA; the modeled radiance and flux constitute a theoretical Angular Distribution Model (ADM relating radiance to flux) for the footprint. Second, a straightforward parameterization based on MODTRAN4 (Anderson et al.) is then applied; the inputs are view zenith angle and radiance. The parameterization maps the 8.0 µm to 12.5 µm Fu-Liou radiance to an "unfiltered" (geophysical) 8.0 µm to 12.0 µm emulated radiance and also to a "filtered" 8.0 to 12.0 µm emulated radiance. Recall that the spacecraft itself observes a filtered radiance, a signal which includes the effect of the spectral response of the instrument. It is the task of SSF to account for the spectral response and produce an unfiltered radiance. In the second step here, the spectral response (filter function) of the instrument is modeled, producing an emulated filtered window radiance; this is CRS-183. Third, the theoretical ADM (based on 8.0 µm to 12.5 µm) converts the unfiltered 8.0 µm to 12.0 µm emulated radiance into an emulated window flux, which is reported as CRS-184. The unfiltered, emulated window radiance is not archived.

While the original Fu-Liou code offered empirical droplet size spectra based on early field campaign data, we now use theoretical, gamma distributions for the radii of cloud water droplets (Hu and Stamnes, 1994), consistent with the Minnis et al. (1998) retrievals on CERES SSF input stream. The code treats all ice cloud crystals as randomly oriented hexagons characterized by a generalized effective diameter Dge. The SSF cloud retrievals also assume randomly oriented hexagons but express them as effective diameter De. Caution is advised when interpreting CRS results for ice clouds, as both the input cloud retreivals (SSF) and the radiative transfer calculations do not account for the enormous variation of crystal shapes found in nature.

The typical CRS calculation uses 30 atmospheric layers with fixed thickness layers of 10 hPa and 20 hPa nearest the surface. The remainder are placed on a sliding scale following the input value for surface pressure. Additional layers, at levels "custom made" for each footprint, are inserted in the radiative transfer calculation for cloud top and cloud bottom. Edition2C CRS places the cloud top as per the pressure top retreived by SSF. The SSF estimate for cloud geometrical thickness is used to specify cloud bottom.

Reflection of SW by Surface

The spectral dependence of surface reflectivity for land surface albedos are specified according to the CERES Surface Properties maps (from CERES/SARB Surface Properties) following Rutan and Charlock (1997 and 1999). CRS uses the Wilber et al. (1999) surface LW spectral emissivity maps (which are available at the same URL). Both SW and LW surface maps are keyed to International Geophysical Biospherical Project (IGBP) land types.

Ocean spectral albedo is obtained using a look up table (LUT) based on discrete ordinate calculations with a sophisticated coupled ocean atmosphere radiative transfer code (Jin et al., 2002, Jin and Stamnes, 1994). Inputs to the look-up table for ocean spectral albedo include cosine of the solar zenith angle (cosSZA), wind speed (from ECMWF), chlorophyll concentration (which has a minor effect on broadband flux), and SW optical depth of clouds and aerosols (from SSF) for the respective spectral interval. There is an empirical correction for surface foam based on wind speed.

For clear footprints during daytime, the broadband surface albedo is explicitly retrieved using TOA observations and iterations of the Fu-Liou code with the constrainment algorithm; the broadband albedo is then simply a ratio of upwelling to downwelling SW at the surface. When a CRS footprint contains clouds, the broadband surface albedo is assumed using the Surface Albedo History (SAH) procedure. The SAH algorithm is run at the start of each month of CRS processing. SAH identifies the clear SSF footprints during the month with the most favorable geometry for the retreival of surface albedo: those with large values of cosSZA. SAH uses a quick table look-up to the Fu-Liou code that relates TOA albedo, surface albedo, cosSZA, precipitable water (PW), and aerosol optical thickness (AOT). Using the nearest 6-hourly AOT from the MATCH aerosol assimilation, the look-up retrieves a first guess surface albedo for the month. This first guess surface albedo corresponds to a clear SSF/CRS footprint. The monthly value for the first guess surface albedo is then written to a SAH file for each of the 10 by 10 minute gridded tiles, whose center points are contained in the clear footprint. Each 10 by 10 minute gridded tile of land is thus given an initial broadband surface albedo for the month. The SAH albedo is stored internally as a reference value A_o using the Dickinson (1982) relationship

$$A(\text{cosSZA}) = A_o(1 + d)/(1 + 2d\ \text{cosSZA})$$

where d is specified for each IGBP type and A_o is the albedo at cosSZA of 0.5. The look-up, first guess values of A_o for the various 10 by 10 minute tiles are then available to construct a fixed broadband surface albedo as an input for radiative transfer calculations with any cloudy footprint, for which we assume A(cosSZA=0.5). When a land footprint is clear during daylight, the surface albedo is explicitly retrieved with the CRS constrainment algorithm by iterating the Fu-Liou code (not as a quick table look up) with ECMWF and MATCH inputs. The quality of the surface albedo retrieval depends heavily on the realism of the MATCH simulation of AOT and the CRS assignment of the corresponding single scattering albedo (see Treatment of Aerosols and Table 2). The most reliable CRS values of surface albedo are expected for clear footprints under high sun, in regions and seasons with low AOT.

The Photosynthetically Active Radiation (PAR) product (CRS-132), which is generated only at the surface, is simply the SW output of Fu-Liou from 437.5 to 689.6 nm. To date, we have not compared CRS-132 with any surface observations.

Treatment of Aerosols

Each footprint accounts for the effect of aerosols on SW fluxes, LW fluxes and 8.0-12.0 µm window fluxes at all levels, and on broadband LW

and filtered window radiance at TOA. The SSF product for 0.63 µm aerosol optical depth (AOT), which is based on cloud-screened VIRS imager data over the ocean, is used when available. Otherwise, we uses visible AOT from the Collins-Rasch MATCH, which is an advanced aerosol assimilation. When lacking MATCH (this is rare), a monthly mean AOT is assumed from the GFDL global aerosol model (courtesy of Brian Soden). The MATCH is available for the TRMM record of January-August 1998, but not for the spotty CERES TRMM record after August 1998. MATCH provides AOT according to 7 types (Table 2) on a 6-hourly basis over the globe for all sky conditions. Sources of aerosol in MATCH include formation from industrial emissions (as a climatology). More timely MATCH AOT inputs include AVHRR-based retreivals over clear regions of the ocean and wind-blown dust. MATCH itself accepts the NCEP analysis as an meteorological input. MATCH advects aerosols and removes aerosols with wet (cloudy) and dry processes. For economy in transferring MATCH files from NCAR, we take on the column AOTs of each type (rather than the profile) and assume vertical scale heights (Table 2).The aerosol type is always taken from MATCH or the GDFL monthly model (first column of Table 2). The selection of types then yields the scale heights and translation from visible AOT to AOT in all other SW and LW bands. The spectral single scattering albedos and asymmetry factors are assumed from the Tegen and Lacis (1996) and OPACS-GADS (Hess et al., 1998; d'Almeida et al., 1991) models. Footprints with significant amounts of Tegen and Lacis 2.0 µm dust and/or OPAC soot will have strong absorption by aerosols in the computed SW. As CRS has coarse vertical resolution (i.e., outputs at surface and 500 hPa), the assignment of scale height should have a small effect on SW in most clear footprints. But if a dust outbreak spreads to say 6 km, the CRS aerosol forcing in the LW will not be realistic at either the surface or at TOA.

Recent studies with AERONET (Dubovik et al., 2002) suggest that absorption is too high in the Tegen and Lacis 2.0 µm dust. If Dubovik et al. are correct, both our computed atmospheric absorption for desert dust and our retrieved desert surface albedos would then be high, too. But dust optical depths in the MATCH assimilation are overwhelmingly of the 0.01-1.0 µm class (Table 2), for which we assign the radius 0.5 µm. Single scattering albedoes for the Tegen and Lacis 0.5 µm dust are closer to the values reported by Dubovik et al.

The user is advised that fluxes based on satellite retreivals of aerosols are not expected to have the relative veracity of say, fluxes based on satellite retreivals of SST. Further caution is advised when an aerosol assimilation (MATCH) or a climatology (GFDL) is employed, as here.

Table 2: Assignment of aerosol characteristics

MATCH aerosol type	CRS aerosol optics	scale height
dust (0.01-1.0 µm)	dust (0.5 µm) Tegen-Lacis	3 km
dust (1-10 µm)	dust (2.0 µm) Tegen-Lacis	1 km
dust (10-20 µm)	dust (2.0 µm) Tegen-Lacis	1 km
dust (20-50 µm)	dust (2.0 µm) Tegen-Lacis	1 km
hydrophilic black carbon	soot (OPAC)	1 km
hydrophobic black carbon	soot (OPAC)	1 km
hydrophilic organic carbon	soluble organic (OPAC)	1 km
hydrophobic organic carbon	insoluble organic (OPAC)	1 km
sulfate	sulfate (OPAC)	1 km
sea salt	sea salt (OPAC)	0.5 km

Results for Clear and Cloudy Footprints

Clear footprints are those having no clouds identified by the VIRS imager (see SSF Collection Guide). For such footprints, TOA radiation parameters (first matrix in Table 1) and clear-sky parameters (third matrix in Table 1) are then adjusted. As simple, raw arithmetic means of the CERES footprints (averages of both day and night for SW and LW, not spatially gridded or time smoothed) for April 1998, the computed and observed fluxes at TOA are within a few Wm^{-2} over the ocean and land (Table 3). Rms differences of Mean adjustments to upper tropospheric humidity (UTH), total precipitable water (PW), and surface temperature over ocean (SST) are small. This indicates that the ECMWF humidity profile, which is based on an assimilation of TOVS radiances (i.e., HIRS/2 on the operational satellites), is consistent with our radiative transfer calculations and CERES observations; and provides some confidence in the CRS LW fluxes at 500 hpa, 200 hPa, and 70 hPa for clear ocean footprints. Over the ocean, the standard deviation (typical adjustment) to AOT is 0.084, which is almost as large as the mean AOT of 0.097 (Table 3). This suggests that the aerosol forcing in CRS (the difference of clear and pristine computed flux outputs) is not consistent, on a footprint by footprint basis, with the forcing that would be inferred from the VIRS (SSF) and MATCH (the aerosol assimilation). The distinction of the CERES, VIRS, and AVHRR instruments must account for some of the difference in aerosol forcing. But we suspect a significant impact by different treatments of ocean optics, which pose another uncertainty (see the CAVE web site and select "CLAMS" for a relevant field experiment). Specular reflection from the ocean surface (sunglint) is highly directional and variable. Effects related to glint generate considerable noise in the SSF inversion of radiance to flux over the clear ocean.

Table 4 shows results for all-sky and overcast footprints. As for the clear footprints, the mean biases to TOA fluxes and adjustments of the radiative transfer parameters are small. But here we show the standard deviations of the adjustments to the key cloud parameters. The standard deviations of the adjustments to cloud visible optical depth are quite large: 27.4 for all sky and 11.5 for overcast. This is due to in part to the adjustments of cloud fields that have high initial optical depth. For example, an initial optical depth of 150 tuned to170 is an absolute adjustment of 20 in optical depth, but a modest fractional change. For a solar zenith angle of 40 degrees, this would increase reflection at TOA by only 4 Wm^{-2}. The standard deviations of difference between untuned, initial calculations for TOA flux and CERES footprint observations are here 17.3 Wm^{-2} for reflected SW and 7.3 Wm^{-2} for OLR, under all sky conditions. A primary achievement of tuning is a factor-of-two reduction of these large instantaneous, footprint scale differences to 9.7 Wm^{-2} for SW and 4.0 Wm^{-2} for OLR, under all sky conditions. Statistics in Tables 3 and 4 are based on both day and night for all parameters. This effectively reduces the bias for SW

parameters. Under daylight only, the all sky SW (observed - untuned) mean bias increases to 1.2 Wm^{-2} (from 0.6 Wm^{-2} in Table 4) and the standard deviation increases to 25.8 Wm^{-2} (from 17.3 in Table 4).

Table 3: Sample of CRS for clear-sky (cloudless) footprints; raw arithmetic means for April 1998, both day and night. Daytime-only errors for SW fluxes are larger than values in table.

	ocean	**land**
TOA fluxes in Wm^{-2}		
SW reflected (observed - untuned)	-0.2	1.6
SW reflected (observed - tuned)	-0.3	0.3
OLR (observed - untuned)	1.1	1.1
OLR (observed - tuned)	0.7	0.9
PW (surface to 500 hPa) in cm		
Input from ECMWF	3.23 cm	1.84 cm
Std. dev. of adjustment by tuning	0.34 cm	0.07 cm
UTH (upper tropos. humidity) in %		
Input from ECMWF	25.9 %	23.0 %
Std. dev. of adjustment by tuning	2.5 %	0.8 %
Aerosol optical thickness (AOT) vis.		
Input from SSF/VIRS or MATCH	0.097	0.156
Std. dev. of adjustment by tuning	0.084	0.000
Surface skin temperature		
ECMWF/NOAA sea, SSF/VIRS land	298.1 K	296.0 K
Std. dev. of adjustment by tuning	0.4 K	2.2 K

Table 4: Sample of CRS for all-sky and overcast footprints; raw arithmetic means for April 1998, both day and night. Daytime-only errors for SW fluxes are larger than values in table.

	All sky	**Overcast**
TOA fluxes in Wm^{-2}		
SW (observed - untuned) as mean/std dev	0.6/17.3	-1.7/17.2
SW (observed - tuned) as mean/std dev	-0.4/9.7	-0.0/8.0
OLR (observed - untuned) as mean/std dev	0.7/7.3	0.6/8.5
OLR (observed - tuned) as mean/std dev	0.2/4.0	0.0/3.4
Cloudiness of footprint		
Input from SSF (VIRS)	54.9 %	99.7%
Adjustment by tuning as mean/std dev	-0.0/2.3 %	-0.0/1.1 %
Cloud visible optical thickness		
Input from SSF (VIRS)	5.2	8.4
Adjustment by tuning as mean/std dev	0.2/27.4	-0.1/11.5

Cloud top temperature		
Input from SSF (VIRS)	267.1 K	257.0 K
Adjustment by tuning as mean/std dev	-0.0/3.3 K	-0.0/4.0 K

The fact that constrainment (or tuning) algorithm does NOT yield a perfect match to CERES at TOA is recalled by Figure 4 covering January-August 1998 (Charlock et al., 2002). For spring 1998, the tuned calculations for SW are further from the CERES observations than the untuned calculations (but tuned LW are then closer to CERES than are untuned LW). Note that the untuned LW fluxes are a few Wm^{-2} larger than the CERES, and the untuned reflected SW fluxes are generally smaller than CERES. The most critical inputs for these calculations are the cloud properties from VIRS (Minnis et al., 2002). Over roughly 40N-40S during this 8 month period, there is an increasing tendency for CERES to both emit more in the LW and to reflect more in the SW, than we see in the untuned calculations; this is the case for clear skies, too (not shown), for which the effect of the VIRS imager on the radiative transfer inputs is minimal.

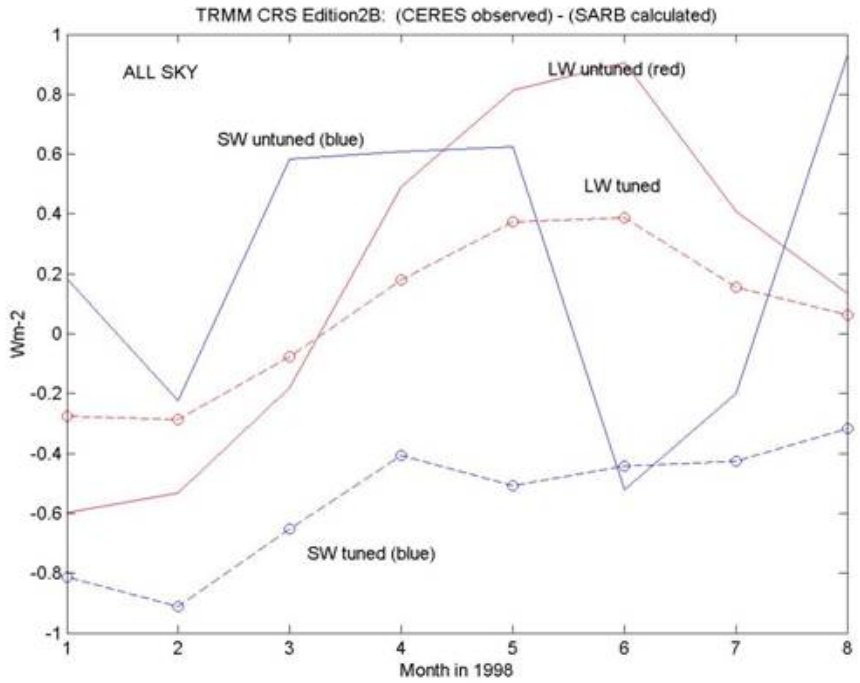

Figure 4. Difference of CERES observations and calculations for TRMM domain (~40S-40N) during January-August 1998 as simple, ungridded means from an enormous number of footprints spanning both day and night.

Comparison with Surface Observations

Retrievals of surface flux are here compared with surface-based observations which are available online through the CERES "ARM" Validation Experiment (CAVE) web site. CAVE (Rutan et al., 2001) provides high quality surface data at over 30 sites worldwide. About half of the sites are part of the ARM Southern Great Plains (SGP) network (Stokes and Schwartz, 1994). Many CAVE sites, such as the SGP Central Facility, and NOAA SURFRAD (Augustine et al., 2000) and CMDL stations, subscribe to the rigorous BSRN observing protocol (Ohmura et al., 1998). Each CAVE surface observation (CAVE Obs) is expressed as a 30-minute mean. We represent the surface flux over the large span of the satellite footprint by using an adjusted time mean of the point surface observation. While surface SW fluxes in the CRS record are "instantaneous" at their respective SZAs, we have adjusted observed SW fluxes in Table 5 with the formula

Obs SW flux in Table 5 = (CAVE Obs SW flux)*[cos(SZAceres)]/[30 min. mean cos(SZA)]

This converts the 30 minute mean observation to a value that represents the surface flux for the satellite observation. Measured values of surface radiation are NOT used in constrainment (tuning). Hence the comparison of fluxes at the surface in Table 5 below is a "cold" test. Observed values of TOA radiation are indeed used in constrainment (tuning), as explained earlier.

Table 5: Comparison of CRS SARB fluxes with observations. CAVE record from surface radiometers at over 30 ARM, BSRN,
and SURFRAD sites (1998). TOA observations from CERES SSF. Here SW fields are daytime means, unlike Table 4.

	Obs Mean Wm^{-2}	**N**	**Bias Obs-SARB Wm^{-2}**	**RMS Wm^{-2}**	**Cloud Forcing Wm^{-2}**
ALL SKY					
LW Down Surface	358	8601	2	19	16

LW Up Surface	429	6780	2	20	
SW Down Surface	443	4990	-34	82	-108
SW Up Surface	91	4162	12	26	
LW Up TOA	252	9282	-0	4	-24
SW Up TOA	219	5158	1	17	89
OVERCAST					
SW Down Surface	236	1220	-28	83	-306
CLEAR VIRS					
SW Down Surface	523	1601	-35	55	
CLEAR VIRS + pyranometer					
SW Down Surface	485	205	-27	68	

Table 5 shows that while the tuned surface fluxes for LW compare very well with observations, tuned surface SW fluxes are far from the mark. The daytime all-sky bias for insolation is -34 Wm^{-2}; this is a daily mean (24-hour) bias of -17 Wm^{-2}. The SSF component of CERES has already released (CER_SSF_TRMM-PFM-VIRS_Edition2B) LW and SW surface fluxes, retreived by simpler and quicker methods than those developed by more complex techniques here in CRS. The SSF surface LW fluxes compare well with observations. Ensemble means of SSF Model B surface SW fluxes, which do not use 6-hourly MATCH for input, are often within 10-20 Wm^{-2} of observations for groups of land stations. Given that CRS SW computations agree well with CERES at TOA for all-sky (Table 5) and clear-sky (Table 3) footprints, what then accounts for the large biases in SW at the surface in the present CRS file?

Firstly, we are confident that most of those large biases in surface SW flux (Table 5) are not due to the modified Fu-Liou code. A rigorous, year-long test of the code for clear-sky SW insolation is summarized in Table 6 (from Charlock et al., 2001). ARM observations in Table 6 are restricted to year 2000 and include only data from the well tended Central Facility (C01) and a second collocated battery of radiometers (E13). In response to reports of discrepancies between calculations and measurements (i.e., Charlock and Alberta, 1996, Kato et al., 1997) and advances in measurement science (i.e., Haeffelin et al., 2001), radiometric observations were upgraded at SGP during 1999. Insolation measured at the SGP in 1998 was reported as ~20 Wm^{-2} lower than in 1999. Note that surface observations in Table 5 are based on 1998 data, and that roughly half of sites are clustered around the SGP. The year 2000 clear-sky test in Table 6 uses satellite input only for the ozone profile; cloud screening was based on temporally intensive time series from the surface radiometers (Long and Ackerman, 2000); AOT was taken from the AERONET Cimel (Holben et al., 1998), and a 10% soot fraction was assumed; soundings were from SGP balloon launches. The bias is low, even for the separate direct and diffuse components (Table 6).

Table 6: Offline (non-CRS) comparison of SW (Wm^{-2})
Model minus ARM SGP Central Facility (sites E13 and C01) during 2000.

	Model - Obs		**Sample N**	**Aerosol Forcing**
Surface	**E13**	**C01**		
Direct normal	-4.1	-10.0	500	-131.3
Diffuse	6.7	5.2	500	58.6
Total	3.3	-2.1	500	-27.5
Direct horizontal =(dir norm)*cosSZA	-3.4	-7.3	500	-86.1
TOA reflected (Obs. here ES8, not SSF)	13.2	27.0	44	

Table 7 for ARM SGP E13 uses the same location as Table 6, where off-line comparisons with Fu-Liou where favorable and we have had more opportunity to examine the integrity of the radiometric record than at all CAVE sites. A check of the ECMWF PW over SGP (where the insolation bias is large) with GOES/AERI and nighttime Raman lidar during July confirms that our PW input is not the main problem in the bias for clear-sky SW insolation in Table 7.

Does cloud screening explain the bias in clear sky insolation? If VIRS has missed some clouds and identified a footprint as clear, the result

would be expected to contribute to a negative bias in clear sky SARB insolation in Tables 5 and 7. In the bottom rows of Table 5 and 8, a more intensive cloud screening is employed; the VIRS cloud imager PLUS the surface radiometric time series. While this more intensive screening reduces the bias in clear sky insolation (from -23 Wm^{-2} to -14 Wm^{-2} in Table 7), this reduction is likely caused by a simple reduction in the mean insolation of the sample (from 512 Wm^{-2} to 324 Wm^{-2}). For ARM SGP E13 (Table 7), CERES cloud screening does not appear to be a significant source of mean bias in clear sky insolation.

Table 7: Comparison of CERES SARB Surface Fluxes with Observations and surface radiometers at ARM SGP E13 (Central Facility) January-August 1998. Here SW fields are daytime means, unlike Tables 3 and 4.

	Obs Mean Wm^{-2}	**N**	**Bias Obs-SARB Wm^{-2}**	**RMS Wm^{-2}**	**Cloud forcing Wm^{-2}**
ALL SKY					
LW Dn Sfc	349	455	-3	18	17
LW Up Sfc	416	430	-3	16	
SW Dn Sfc	423	260	-21	60	-106
SW Up Sfc	87	260	11	20	
LW Up TOA	247	457	0	4	-27
SW Up TOA	225	260	2	8	88
OVERCAST					
SW Dn Sfc	243	68	-27	87	-309
CLEAR VIRS					
SW Dn Sfc	512	94	-23	29	
CLEAR VIRS + pyranometer					
SW Dn Sfc	324	17	-14	17	
SW direct			-5		
SW diffuse			-9		

Some of the bias in the clear-sky SW can be ascribed to aerosol forcing. The input AOT over land is taken from the MATCH assimilation. A plot from the 23-25 January 2001 CERES STM showed the January-August 1998 AOT at SGP for MATCH (0.12) and AERONET (0.20). This suggests that the aerosol forcing in CRS at SGP could be low by almost a factor of 2. For the clear sky insolation bias of -23 Wm^{-2} in Table 7, the corresponding aerosol forcing computed with MATCH AOT is -16 Wm^{-2} (see "Site by Site Statistics" at the CAVE web site). Note that over land, while MATCH relies heavily on climatological sources for aerosol, the year 1998 at SGP saw an extraordinary impact due to smoke from fires in Mexico. AERONET reported almost twice as much aerosol during summer at SGP in 1998 versus 2000. Note that when compared with 14 sites (only one of which was at the ARM SGP) during January-August 1998, MATCH (0.16) was then closer to the AERONET (again 0.20).

Tables 5 and 7 give a perspective on other CRS surface products, like surface albedo (the ratio of upwelling to downwelling flux) and LW upward longwave flux (ULF). Note that upwelling SW at the surface is systematically below the observations, both for all sky and clear sky in Tables 5 and 7. This is at first surprising because the downwelling SW in the model, which is the source for the upwelling, exceeds the observations. Hence the surface albedos retrieved here are indeed below the albedos observed at the 10m towers. We suspect that the point-based radiometric observations of surface albedo do not represent the albedo over the large CRS footprints. The towers are typically placed in fenced yards (i.e., no crops or grazing by domestic animals). The impact of such fencing is suggested by the off-line calculations of Table 6, which (unlike the CERES products in Tables 5 and 7) uses the point radiometric observation of surface albedo as an INPUT for the radiative transfer code. Employing both point measured albedo and AOT, the computed reflection at TOA is then substantially higher than CERES ES8 observations (last row in Table 6), suggesting that footprint-wide surface albedos are lower than those over fenced radiometers. Also note that computed reflected SW at TOA, based on inputs from radiometers separated by only a few m at the surface, differ considerably (Table 6).

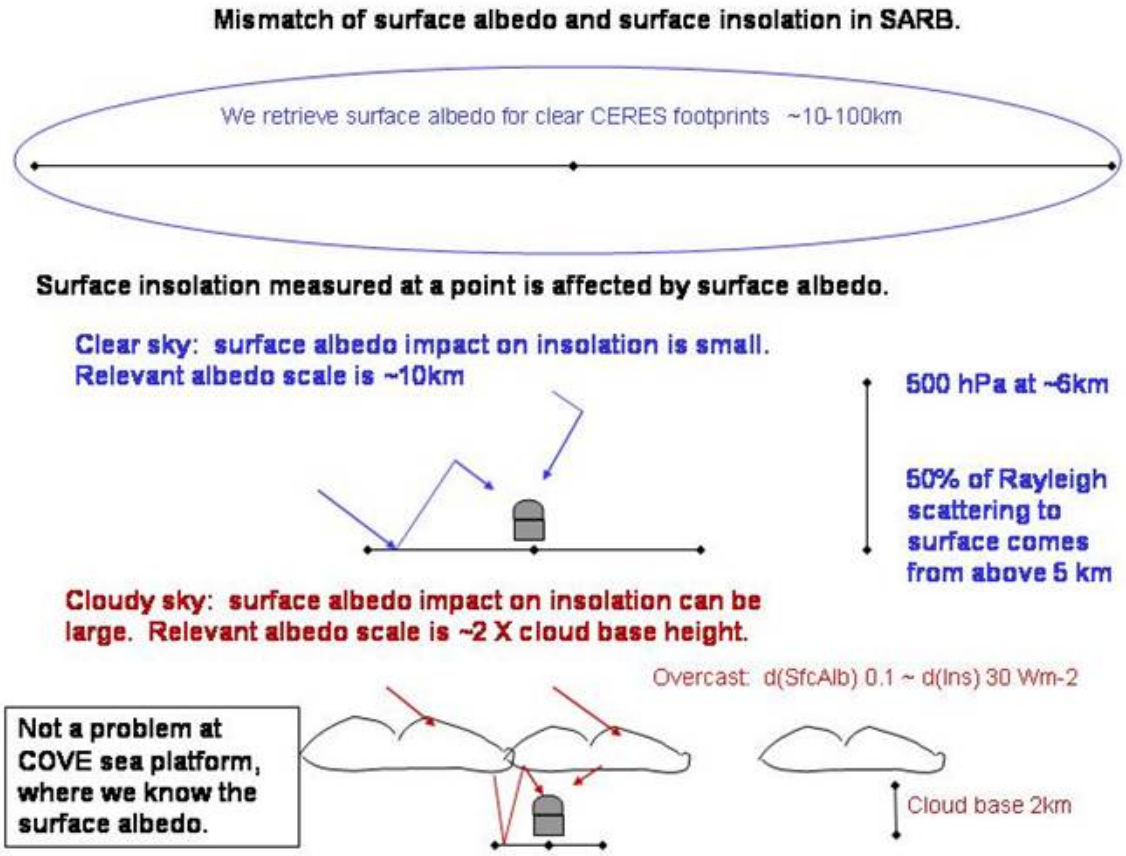

Figure 5 Impact of surface reflection on retrieved surface insolation

If surface albedoes in the immediate vicinity of the measurement sites are systematically lower than those over the larger scale of a CERES footprint, this would explain some of the bias between retrieved and observed insolation. Such effect of secondary reflection on insolation is illustrated in Figure 5. For clear conditions, the impact is small. But under cloudy conditions, secondary reflection is much larger. For a fixed value of reflected flux at TOA, an increase in surface albedo by 0.1 (i.e., changing albedo from 0.15 to 0.25) can increase the downwelling insolation by 30 Wm^{-2}. And if cloud base is low (i.e., 2 km), the effective area for secondary reflection is small (i..e., 2km x 2 km). CRS does not retrieve the surface albedo of such small, 2km x 2km areas. Rather, we use the surface albedo which was retrieved by the much larger CERES footprint under clear skies (top of Figure 5).

Fencing should have a corresponding impact on point observations of upward LW at the surface. As the variation of surface LW emissivity is much smaller than that of SW albedo, one supposes such "representation" (i.e., fencing) bias for upwelling surface LW should be smaller than for SW. But the vegetation canopy has subtle impacts on some satellite products. The current generation of CERES SSF and CRS products do not fully account for the shading of sunlight by vegetation or terrain over land. During the morning, some westward facing surfaces will appear to be in shadow when seen from space by a satellite located to the west of a particular land target. In addition to appearing darker in SW, shaded regions will have reduced skin temperature and thus emit less in the thermal IR. A satellite observing the target from the west will find darker (SW) and cooler (LW) radiances than will a satellite viewing from the east. While any target region has a single set of SW and LW fluxes, the present CERES products are expected to have slight biases of opposite signs, when viewing from the east as opposed to the west.

The outstanding features of Tables 5 and 7 are the large biases in retrieved insolation at the surface. We assume that the bias in clear sky insolation is largely due to aerosol forcing. About 5Wm^{-2} of the bias is due to the radiative transfer code, the latest version of which (Rose and Charlock, 2002) has not been implemented in CRS Edition2C. We speculate that additional bias in all-sky conditions is due to surface albedo (i.e., the albedo near the radiometers is larger than the albedo over the complete footprints, or we have incorrectly implemented a parameterization for surface albedo in cloudy conditions). Data from Cheaspeake Lighthouse and Aircraft Measurements for Satellites (CLAMS) field campaign and the CERES Ocean Validation Experiment (COVE) sea platform will enable a vigorous test of these hypotheses with Terra.

1D Radiative Transfer for a 3D Globe

This product is based on an observed TOA record from SSF with a surface reference level. For example, TOA fluxes referenced to a level surface of the Earth would be 1% larger $(6430/6400)^2$ than TOA fluxes referenced to 30km. At this writing, the effective SSF reference levels for SW and LW are regarded as 20km. This is a 3D radiative transfer problem. It involves the thermal emission and solar tranmission of radiation from the Earth's annulus - footprints that may not even intersect the surface of the Earth. The user is advised that the SARB product, which is generated by 1D radiative transfer, has inherent limitations. The flux product does not reconcile the inherent divergence of radiation from the surface to other altitudes (i.e., the areas of the surface at r~6400km and 70 hPa at r~6418.5km differ by 0.58%).

In global change studies, climate forcing is often assessed at the base of the stratosphere, rather than at TOA. The product here includes fluxes at the surface, 500, 200, 70 hPa, and TOA. Our immediate goal is to achieve accuracy for short term perturbations due to clouds,

aerosols, surface albedo, and water vapor at these levels. From a climate perspective, the product now definitely lacks the accuracy to be applied in an assessment of long term heating and cooling of the Earth (i.e., Levitus et al. and their ~0.25 Wm^{-2}). Such limitations will likely continue, even when more advanced CERES TISA products smooth the results in space and time.

Cautions and Useful Hints

Informal timely additions to this document will be posted at the CAVE web site under "CRS Advice".

1. A coding error set CRS parameters to fill values for approximately 60% of the nighttime CERES footprints during January, February, and March of 1998. We list below the percentage of CERES footprints for which the CRS code ran successfully.

1998	Day+Nite	Nite
Jan	65.58%	38.04%
Feb	66.05%	38.69%
Mar	66.76%	40.05%
Apr	91.63%	94.08%
May	95.18%	97.80%
Jun	94.52%	97.48%
Jul	94.84%	97.66%
Aug	95.03%	97.67%

   The later months typically have CRS for 95% of CERES footprints. For the remaining 5% of footprints, CRS did not run or contained fill values for various reasons; such as a lack of observed TOA fluxes from SSF, SARB radiative transfer aborting due to extreme values for input parameters, or excessive, non-physical adjustments suggested by the constrainment (tuning) algoroithm.

2. The radiative forcing of two aerosol constituents, hydrophilic organic carbon and hydrophobic organic carbon, have been neglected because of an coding error. This error reduces the visible AOT by about 10-15%, with relatively larger effect in regions with signficant biomass burning. In an off line sample calculation of 100,000 daytime fields of view (FOV) over clear ocean, the aerosols forcings WITH the error were

   SW TOA = 8.47 Wm-2 SW Surface = -15.67 Wm-2

   and those WITHOUT the error were

   SW TOA = 9.70 Wm-2 SW Surface = -17.68 Wm-2

   The SARB in CRS Edition 2C has the error. The error does not affect the calculation of pristine (aerosol free) fluxes or the observation (on SSF) of TOA flux. The assignments of aerosol type in Table 2 are based on the MATCH aerosol assimilation, which generally gives higher visible AOT for hydrophilic organic carbon than for hydrophobic organic carbon. Hydrophobic organic carbon aerosols are strong absorbers of SW.

3. For any footprint having a non-zero value for CRS-204 (number of tuning iterations), the untuned fluxes at both surface and TOA can be produced from

   untuned flux = tuned flux - adjustment

   as CRS has values for tuned ("constrained") fluxes and adjustments ("constrained-initial flux deltas") at surface and TOA.

   For example, CRS-149 (SW flux - upward for total sky) has a dimension of 5, yielding values for tuned ("constrained") upward SW flux at TOA, 70 hPa, 200 hPa, 500 hPa, and the surface. CRS-174 (SW flux adjustment at TOA - upward for total-sky) has a dimension of 1, yielding a value for the "constrainment- initial flux delta". The initial, untuned calculation (first run of Fu-Liou code for footprint) of SW flux at TOA is then

   untuned SW flux at TOA = (TOA component of CRS-149) - (CRS-174)

   The tuned (constrained) values for adjustable parameters like cloud top temperature and surface skin temperature (second and third panels of Table 1) can are then

   tuned parameter = initial parameter + adjustment

   For example, using CRS-197 (skin temperature - initial) and CRS-198 (skin temperature - adjustment)

   tuned skin temperature = (CRS-197) + (CRS-198)

4. BEWARE of footprints having zero value for the number of CRS tuning iterations. Fewer than 1% of footprints have values of zero. When the number of CRS tuning iterations has zero value, rule #3 above (the third Caution and Useful Hint) does not apply and

    a. the slot labled as tuned ("constrained") flux actually contains the initial, untuned flux;
    b. the slot labled as flux adjustment (constrainment-initial flux delta) contains BOGUS numbers;
    c. the initial values for parameters OTHER THAN FLUXES (second and third panels of Table 1), like cloud top temperature and surface skin temperature, are useable;
    d. the adjustments for parameters OTHER THAN FLUXES (second and third panels of Table 1), like cloud top temperature and surface skin temperature, are BOGUS.

    For example, if the number of CRS tuning interations is zero

    - the slot for tuned SW flux has values of UNTUNED flux;
    - the slot for adjustment of SW flux has a bad value (don't use it);
    - the value for "skin temperature - initial" (which is not a flux) is okay;
    - the slot for "skin temperature - adjustment" has a bad value (don't use it).

5. The spectral interval for the window is not consistent in all CRS products. The official CERES window (WN) spans 8.0 μm to 12.0 μm (1250 cm^{-1} to 833.333 cm^{-1}). The TOA observed SSF window products use this interval, as do the TOA emulated window products on CRS. But the CRS vertical profiles (CRS parameters having dimension of 5 for the sequence representing the surface, 500 hPa, 200 hPa, 70 hPa, and TOA) of window flux use a DIFFERENT spectral interval, 8.0 μm to 12.5 μm (1250 cm^{-1} to 800 cm^{-1}). See Section on Radiative Transfer Code.

6. Users with interest in a highly accurate estimate of aerosol forcing over the ocean should note that all SW fluxes here computed (pristine, untuned, and tuned) are dependent on the optical properties assumed for the ocean surface. Ocean optical properties are uncertain - both our broadband calculations and in the AOT retreivals that we use. See Jin et al. (2002) for an assessment with a sophisticated model and high quality observations. Updated ocean optics from the Chesapeake Lighthouse and Aircraft Measurements for Satellites (CLAMS) are forthcoming. See Reflection of SW by Surface in this document and the CAVE web site under "CLAMS".

7. Those seeking the most accurate land surface albedos should obtain them from clear footprints under high sun, in regions and seasons with low AOT. See Reflection of SW by Surface section.

8. The product for Photosynthetically Active Radiation (PAR) has not been validated. See Reflection of SW by Surface section.

9. The user may compute aerosol forcing to the surface and TOA by differencing SARB products for pristine and clear skies. The absorption of SW by aerosols, which is highly uncertain, is strongly influenced by the aerosol properties we have taken from the MATCH aerosol assimilation. See sections on Results for Clear-Sky Footprints, and Comparison of CRS with Surface Observations.

10. The retreival of LW at the surface appears to be of good quality. While the SARB WG has some confidence in the quality of retrievals of surface SW over the huge spatial domain of TRMM, the comparison with CAVE point observations is disquieting.

11. Cautions on the use of these preliminary results for global change studies or comparison with measurements in the middle atmosphere are in the section 1D Radiative Transfer for a 3D Globe.

12. The NWP analyst should be wary of the CRS Edition2C retreival of UTH (or more properly, adjustments to the UTH from our ECMWF input). The UTH from ECMWF is based partly on TOVS data at 6.7 μm. The CRS adjustment of UTH is based more crudely on differences between broadband LW and 8.0-12.0 μm window radiances. The UTH inferred is then influenced more heavily by optical properties assumed for the window and the far IR, which are more uncertain than at 6.7 μm. CRS Edition2C uses the CKD 2.4 continuum. Surface skin temperature also plays a role in the CRS retreival of UTH. Experimentation has shown that use of an ocean skin temperature from TMI would improve our simulation of clear sky LW.

13. Focused studies on sunglint at COVE (Su et al., 2002) point out how hard it is to parameterize the highly directional reflection of SW from the ocean under clear conditions. Sunglint introduces considerable noise to the OBSERVED flux at TOA, which CERES inverts from measurements of radiance at specific angles. It can increase or decrease the "observed" flux for specific clear and partly cloudy footprints. While SSF screens for sunglint when retrieving AOT and cloud properties that are used for inputs to CRS, such screening is not perfect. One measure of the fidelity of observations and theory is dispersion, here regarded as the rms difference of observation and theory divided by the mean value of the observation. Over the ocean, the dispersion for reflected SW at TOA is higher for clear conditions than for all-sky conditions. The higher dispersion for clear conditions is produced by sunglint. Sunglint is the bane of many instantaneous footprints. When averaging over sufficient time and viewing geometry, its effect mostly goes away.

14. An update to the modified Fu-Liou code with more recent line parameters is in progress. This may reduce the surface insolation by about 5 Wm^{-2}. It will be used for new Terra processing.

15. A software error caused the value for CRS-135, the number of atmospheric levels, to be stored as garbage for each footprint. Users may safely substitute a constant value of 5 for the value obtained from the product. This error has been corrected for future versions of the CRS product.

Accuracy and Validation

Accuracy and validation discussions are found in the following sections of Nature of the CRS Product.

- Results for Clear and Cloudy Footprints
- Comparison with Surface Observations
- 1D Radiative Transfer for a 3D Globe

The numbered items of Cautions and Useful Hints also address accuracy and validation.

References

- List of CERES CRS References

Expected Reprocessing

In the longer term, yet more advanced versions of CRS are expected. A future run will use a "frozen" NWP analysis. There will be advances in the TOA fluxes. SSF will use new techniques to identify multilayer clouds. For an indefinite time, however, we anticipate continuing, significant uncertainties in CRS products for

- surface SW and atmospheric absorption of SW because of mixed phase clouds (land and sea), aerosol single scattering albedo (land and sea) and AOT (land);
- LW fluxes at the surface and at 500 hPa because of multiple layer clouds (land and sea).

Referencing Data in Journal Articles

The CERES Team has gone to considerable trouble to remove major errors and to verify the quality and accuracy of this data. **Please provide a reference to the following paper when you publish scientific results with the CERES TRMM Edition2C CRS data:**

Wielicki, B. A., B. R. Barkstrom, E. F. Harrison, R. B. Lee, G. L. Smith, and J. E. Cooper, 1996: Clouds and the Earth's Radiant Energy System (CERES): An Earth Observing System Experiment. Bull. Amer. Meteor. Soc., 77, 853-868.

When Langley ASDC data are used in a publication, **we request the following acknowledgement be included:** "These data were obtained from the NASA Langley Research Center EOSDIS Distributed Active Archive Center."

The Langley ASDC requests two reprints of any published papers or reports which cite the use of data that we have distributed. This will help us determine the use of data that we distribute, which is helpful in optimizing product development. It also helps us to keep our product references current.

Feedback

For questions or comments on the CERES Quality Summary, contact the User and Data Services staff at the Atmospheric Science Data Center.

Informal contact to the SARB WG is accessible by selecting "The Group" at the CAVE web site.

Document Creation Date: February 21, 2003
Modification History:
Most Recent Modification: